Arch. Metall. Mater. **66** (2021), 4, 1149-1156

DOI: 10.24425/amm.2021.136435

W. KOWALSKI[1*], H. PAUL[1], P. PETRZAK[1], Ł. MAJ[1], I. MANIA[1], M. FARYNA[1]

INFLUENCE OF HOT PRESSING ON THE MICROSTRUCTURE OF MULTI-LAYERED Ti/Al COMPOSITES

Metal-intermetallic layered (MIL) composites attract considerable attention due to their remarkable structural and ballistic performance. This study aimed to develop a Ti/Al-based multilayered MIL material by adding ceramic powders, since they can improve the composite's impact resistance. To this end, an experiment was conducted which a stack of alternating Ti and Al sheets bonded by hot pressing; Ti/Al multilayers containing additional layers of Al_2O_3 and SiC powders were also produced. The samples obtained were examined using electron microscopy techniques. The clads' mechanical properties were investigated using a Charpy hammer. In the reaction zone, only one intermetallic phase occurred: the Al_3Ti phase. The model with an additional Al_2O_3 layer showed the highest impact energy. None of the Ti/Al clads broke during the Charpy impact test, a result proving their high ductility.

Keywords: Ti/Al multilayers, electron microscopy, impact test

1. Introduction

MIL composites based on a lightweight Ti-Al system have become the most frequently investigated group of materials for future ballistic applications, thanks to their enhanced impact resistance. Intermetallic phases formed as a result of an Al and Ti reaction have considerable mechanical strengths. For example, the Al_3Ti phase shows a hardness of about 5500 MPa, and its formation has been shown to significantly improve the mechanical strength of the resulting composite material [1-2]. Joining different Ti and Al materials is difficult using conventional welding methods, especially in the case of multilayered materials, because Ti and Al significantly differ in terms of melting temperatures. Researchers have thus been trying to develop methods that are both efficient and low-cost.

Until now, Ti/Al-based MIL materials have usually been produced through joining solid-state metals, using such methods as explosive welding [1-4], hot roll-bonding [5-6], and hot pressing [7-8]. Explosive welding employs high pressure and deformation rates, an approach inducing the formation of a wavy interface with intermetallic phases that due to the oblique collision of the plates are enclosed in vortices [1-4]. In laminate composites obtained by hot roll-bonding [5-6], clads need to be isothermally heat treated before pack rolling, in order to reduce deformation resistance. This process makes the hot roll-bonding technology high-cost and overly complex. A more promising method to produce Ti-Al laminate composites with a controlled microstructure, high bond integrity, and minimal oxidation is hot pressing under a moderate pressure. If the process is carried in air atmosphere that is, without vacuum a decrease in costs is evident.

Hot pressing bonds specific Al-Ti sheets. In the experiment conducted by Fan et al. [7] samples were prepared by hot pressing in vacuum (10^{-3} Pa) at 773, 823 and 873 K for three hours under a pressure of 5 MPa. The intermetallic phase did not form in Ti/Al laminate composites prepared at 773 and 823 K, while the Al_3Ti intermetallic phase formed in composites prepared at 873 K. A similar experiment was conducted by Tao et al. [8], in which Al and Ti sheets were bonded in vacuum (10^{-3} Pa) at 823 K under a pressure of 5 MPa for three hours, but then the samples were furnace cooled to room temperature. SEM and XRD analyses showed no intermetallic compounds formed at the interface at 823 K. Since hot pressing opens a way to modify the microstructure and mechanical strength of Ti/Al MIL composites, thanks to introducing additional layers like these containing ceramic particles, the process can produce new complex phases.

Ti-Al composites can be reinforced by adding SiC ceramic particles, as shown by Wang et al. [9]. A diffusion-reaction between Ti and Al-SiC samples containing 70% SiC particles was tested under bonding temperatures from 873 to 1173 K, a holding time from 0.5 to 6 hours, and pressures from 5 to 15 MPa. The SEM/EDX and X-Ray diffraction analyses of the Ti-Al-SiC composite pressed at 873 K for 1.5h/10 MPa did not reveal

[1] INSTITUTE OF METALLURGY AND MATERIALS SCIENCE, POLISH ACADEMY OF SCIENCES, 25 REYMONTA STR., 30-059 KRAKÓW, POLAND.

* Corresponding author: w.kowalski@imim.pl

an intermetallic phase. When pressing temperature increases, $Ti_7Al_5Si_{12}$ is formed at 873 K, and Al_3Ti and $Ti_7Al_5Si_{12}$ are formed in the range of 973-1173 K. No one, however, has published on investigations into Ti/Al MIL composites strengthened with other ceramic materials, like Al_2O_3 or nanoparticles of SiC.

This research aimed to use hot pressing under air atmosphere to develop a Ti/Al-based MIL multilayer material, strengthened with additional layers of ceramic materials (Al_2O_3 and SiC) applied in the form of powders with different grain sizes. This study also aimed to analyze whether employing additional ceramic powders affects the growth of the intermetallic phase and the impact strength of the resulting composite and whether the type and grain size of the powder makes a difference. Therefore, this research studies if such a method is effective. If it is, then it is likely to offer a new efficient alternative to the methods currently used, since using hot pressing under air atmosphere, instead of vacuum or gas atmosphere, can significantly reduce the cost and complexity of investigations.

2. Material and methods

The hot pressing method used Ti (Gr1) and Al (AA1050) sheets. The bonded materials were divided into three sets of samples. The first set (denoted as S-samples) was made from eight square-shaped Al and nine square-shaped Ti plates of 13×13×0.5 mm (length×width×thickness) (Fig. 1a); the second set (U-samples), from plates of 55×55×1 mm (eight Ti and seven Al plates) (Fig. 1b); and the third set (V-samples), from samples made with 21 thin Al foils of 55×55×0.03 mm, and 22 Ti plates of 55×55×0.5 mm (Fig. 1b). The U- and the V-samples were prepared especially for mechanical examinations – that's why the plates with 55 mm side length was used. The S-samples with 13 mm side length was prepared only for microstructure observations.

In order to remove oxide layers and other contaminants, both Al and Ti plates but not thin Al foils were ground with abrasive papers of up to 600 grit size, and then cleaned in acetone and rinsed in ethanol. Thin aluminum foils used in the V-samples were cleaned using 10% NaOH water solution, then washed in 65% water solution of HNO_3, and finally rinsed in water and ethanol. To strengthen the material in the U- and V-samples, a layer of ceramic powder was added between the Ti and Al plates. Three powder types were used: (i) Al_2O_3 with a grain size of about 10 μm, (ii) coarse-grained SiC with a grain size of 35 μm, and (iii) SiC nanopowder with a grain size of about 60 nm. A 15% suspension of ceramic powder in ethanol was sprayed on plate surfaces; once the ethanol evaporated, the plates were stacked in alternating layers. Next, they were alternately stacked in a furnace (with Ti plates being placed at the top and bottom layers) and pressed with a load of 59 MPa at 823, 873, 893 and 903 K for 1, 2, 5 and 10 hours (the S-samples) and 7 MPa at 903 K for 5 and 10 hours (the U- and V-samples). Table 1 summarizes the dimensions of the materials and the hot-pressing conditions used. After hot pressing, the samples were prepared for the microstructure observations with electron microscopes: they were cut off into two pieces, ground with abrasive papers of grit sizes ranging from 600 to 7000, and polished with a diamond suspension of 3 μm and 1 μm particle sizes.

Microstructure observations were done in microscale with scanning electron microscopy (SEM), and in nanoscale with transmission electron microscopy (TEM) and selected area electron diffraction (SAED). SEM analysis used a Philips XL30 microscope in the backscattered electrons mode (the SEM/BSE technique), operated at 20 kV. TEM analysis used a FEI Tecnai G2 200 kV FEG microscope equipped with a Fischione High-Angle Annular Dark Field (HAADF) detector for STEM observations, and an EDAX EDX spectroscope. Thin lamellas for TEM/SAED investigations were obtained from the central part of the bonded materials, so that intermetallic zones and initial Al and Ti sheets were covered; these analyses used a FEI Quanta 3D 200 Focused Ion Beam microscope equipped with an Omniprobe lift-out system.

Based on SEM and TEM microstructure images, the dependence of layer thickness and the time of annealing at a certain temperature was assessed using the following formula:

$$d = kt^n \tag{1}$$

where d is the mean layer thickness, k is the growth rate constant, t is the annealing time, and n is the exponential factor [4].

TABLE 1

Construction characteristic and heat parameters of the Al-Ti-ceramic multilayered composites

Sample	Number of intermetallic layers	Ti plate thickness [mm]	Al plate thickness [mm]	Ceramic powder layer; average size of grains	Annealing temperature [K]	Annealing time [h]
S	16	0.5	0.5	—	823, 873, 893, 903	1, 2, 5, 10
U0	14	1	1	—	903	5
U1	14	1	1	Al_2O_3 ~10 μm		5
U2	14	1	1	SiC ~35 μm		5
U2n	14	1	1	SiC ~60 nm		5
V0	42	0.5	0.03	—		5
V1	42	0.5	0.03	Al_2O_3 ~10 μm		10
V2	42	0.5	0.03	SiC ~35 μm		10
V2n	42	0.5	0.03	SiC ~60 nm		5

To analyze how good these theoretical predictions occurred in practice, a linear regression of the experimental results against the corresponding theoretical predictions was employed. The strength of this relationship was represented by the coefficient of determination (R^2), with its value of 1 (or 100%) indicating a perfect fit, and so a perfect theoretical prediction.

Impact tests used a Charpy hammer for the U- and V-samples, with an impact strength being determined for samples without v-notch. The samples were cut-off from the middle of the bonded material (Fig. 1b) and then ground with abrasive papers (grit size of 220) to obtain a stripe about 5 mm wide. Three specimens of each sample were used for the test to get a better precision. The tests were performed at room temperature (around 295 K), with an applied energy of 450 J. The impact energy E_{imp} was determined after each experiment.

3. Results and discussion

3.1. SEM and TEM microstructure observations

Figures 2-3 shows SEM/BSE microstructure images, presenting the cross-sections of the Ti/Al multilayers subjected to hot pressing. In all the samples annealed in temperatures ranging

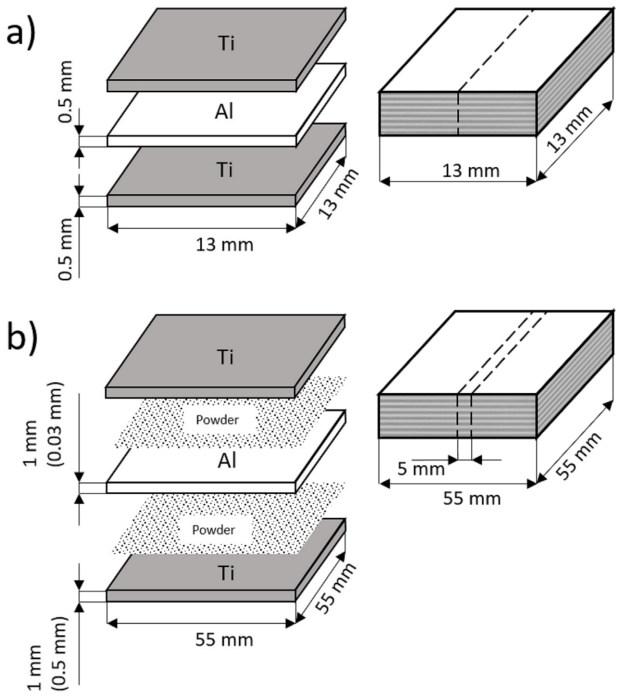

Fig. 1. The scheme for Al-ceramic-Ti multilayer clads for hot pressing: a) samples for microstructure examination (1st set – the S-samples), b) samples for Charpy impact test (2nd set – the U-samples and 3rd set – the V-samples). The dashed line shows the place of cutting

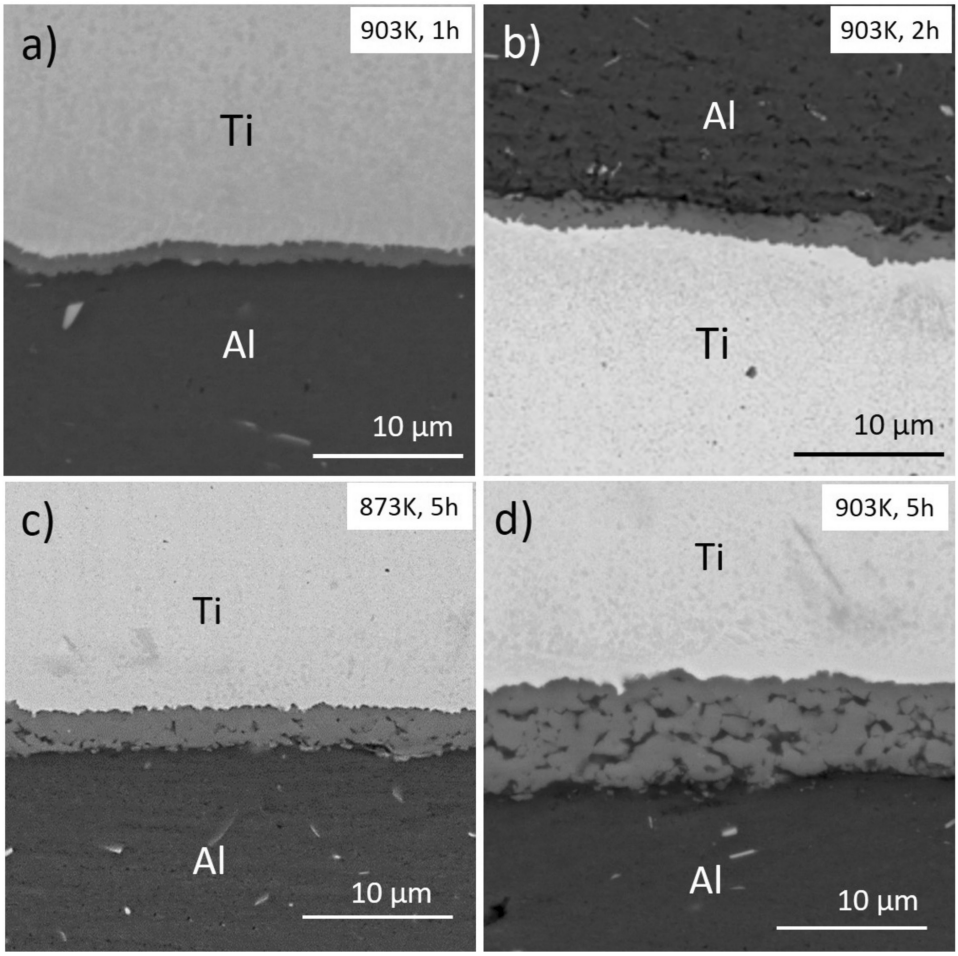

Fig. 2. The SEM/BSE images of the Al-Ti clads showing the microstructure evolution of the intermetallic layer. Pictures were taken from the central part of the sample (6th interface)

from 823 to 903 K, the intermetallic layer was formed near all the interfaces. This layer's thickness increased with time and annealing temperature. After the shortest annealing time (1 hour), at 903 K, the structure of the intermetallic phase was dense and homogeneous (Fig. 2a). Longer annealing times resulted in the formation of dark contrast areas inside the intermetallic layer (Fig. 2b-d). Those dark contrast areas started to appear after annealing at 903 K for 2 hours (Fig. 2b) and at 873 K for 5 hours (Fig. 2c). Annealing at 903 K for 5 hours resulted in the formation of a wide intermetallic layer (Fig. 2d). Increasing annealing time to 10 hours led to a further increase in the thickness of the intermetallic layer, but also to creating an additional, island-like region of the intermetallic phase (Fig. 3). Similar dark contrast areas have been observed in Ti/Al diffusion couples, for example, by Bataev et al. [1] and Fronczek et al. [4].

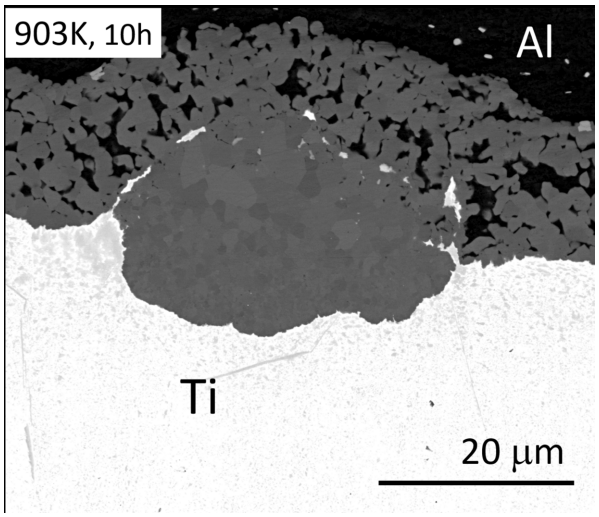

Fig. 3. SEM-BSE image presenting the microstructure of the intermetallic phase of the 6th interface of Al-Ti sample annealed for 10 h at 903 K

Table 2 shows mean layer thicknesses, and Table 3 and Fig. 4 the growth kinetics of the intermetallic phase. The growth rate constant ranged from about 0.5 µm/h^n in 823 K to 2.3 µm/h^n in 903 K. Regression analysis showed that the theoretical prediction using an exponential curve was good in all the scenarios, although it was much better for higher (with R^2 close to 1) than for lower (with R^2 about 0.80) temperatures (Table 3).

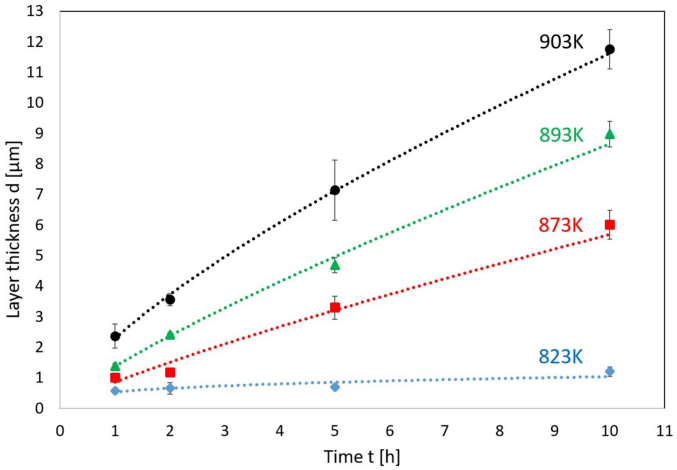

Fig. 4. Dependence of the intermetallic layer's average thickness on the annealing time and temperature

The STEM image shows the structure of the intermetallic layer, composed of nearly equiaxed grains of about 700 nm in size (Fig. 5). The structure was homogeneous in the sample annealed for 1 hour (Fig. 5a). The dark contrast areas found before on the SEM micrographs in the sample annealed at 10 hours (Fig. 2d, 3) occurred to be Al grains, which was confirmed by EDX measurements (Fig. 5c, d).

TABLE 2

The average thicknesses d of intermetallic layers according to the SEM-BSE measurements. ρ is the standard deviation

t	T [K]							
	823		873		893		903	
[h]	d [µm]	σ [µm]	d [µm]	σ [µm]	d [µm]	σ [µm]	d [µm]	σ [µm]
1	0.57	0.06	1.00	0.05	1.37	0.09	2.36	0.39
2	0.65	0.19	1.18	0.12	2.40	0.07	3.55	0.20
5	0.69	0.07	3.29	0.38	4.68	0.25	7.14	0.99
10	1.20	0.15	6.01	0.47	8.97	0.42	11.8	0.65

TABLE 3

Growth kinetics of Al3Ti intermetallic phase. T – the temperature of annealing, k – the growth rate constant, n – the exponential factor, R^2 – the coefficient of determination

T	k	n	R^2
[K]	[µm/h^n]		
823	0.53	0.29	0.79
873	0.85	0.82	0.96
893	1.36	0.8	0.99
903	2.28	0.7	0.99

Intermetallic layers are formed thanks to reaction controlled and diffusion mechanisms [2]. Ti atoms can diffuse to an Al plate, with the diffusion speed depending mainly on the annealing temperature. The temperature of annealing is close to the melting temperature of Al, so the Ti atoms can easy diffuse to the Al crystal lattice. Initially, when the intermetallic layer is very thin, the reactivity of the Ti surface is realized to be to the full extent. It is happened because the supply of the Al atoms is almost instantaneous due to the negligibly short diffusion paths. After sufficient growth in the intermetallic layer, diffusion becomes

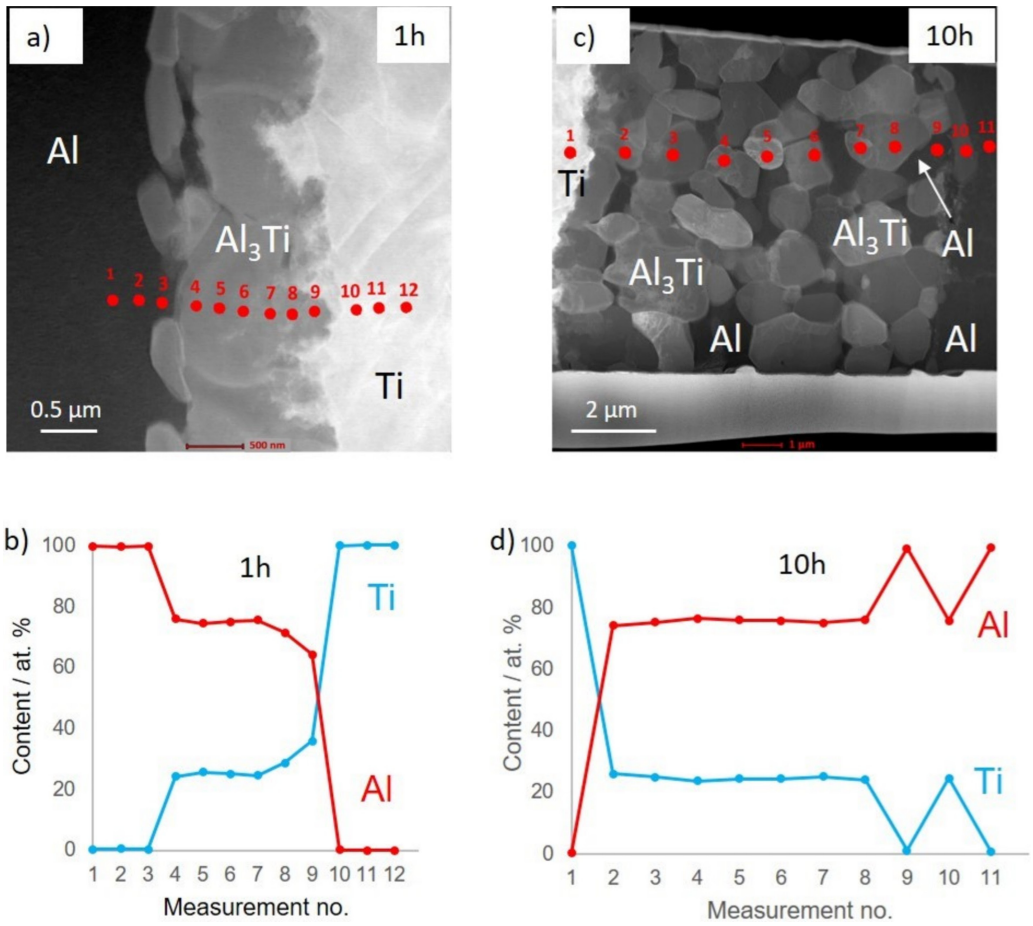

Fig. 5. STEM images presenting the microstructure of 7th interface (central part) of Al-Ti samples annealed at 903K for a) 1 and c) 10 h and b, d) the drawings showing EDX scan obtained from the points highlighted on STEM images

more difficult and will be the controlling step. Further increasing the annealing temperature, however, results in the diffusion of Ti atoms from the intermetallic phase to the Al plate: this makes the intermetallic layer still thicker, but because of the lack of Ti atoms, Al grains appear inside the intermetallic layer (Fig. 5c, d).

The measurements of the EDX point chemical composition (Fig. 5b, d) were carried out across the reaction zone. In both samples did the measurements reveal that the atomic ratio of Al to Ti was close to 3:1 (around 75 at.% Al, and around 25 at.% Ti), which corresponded to the Al_3Ti phase (Tables 4-5). The existence of Al_3Ti was confirmed by the TEM/SAED analysis (Fig. 6). The above results showed that Al_3Ti was the only intermetallic phase that formed at the interface between Ti and Al sheets during hot pressing at 903 K. As was described by Foadian et al. [2] Al_3Ti has the lowest Gibbs standard free energy of formation among the compounds Ti_3Al, TiAl, and

TABLE 4

Chemical compositions of measured points from Fig. 5b

Point	Al at.%	Ti at.%
1	99.7	0.3
2	99.5	0.5
3	99.7	0.3
4	75.8	24.2
5	74.4	25.6
6	74.9	25.1
7	75.5	24.5
8	71.4	28.6
9	64.2	35.8
10	0.1	99.9
11	0	100
12	0	100

TABLE 5

Chemical compositions of measured points from Fig. 5d

Point	Al at.%	Ti at.%
1	0	100
2	74.1	25.9
3	75.1	24.9
4	76.4	23.6
5	75.8	24.2
6	75.7	24.3
7	75	25
8	76	24
9	75.3	24.7
10	75.6	24.4
11	99.5	0.5

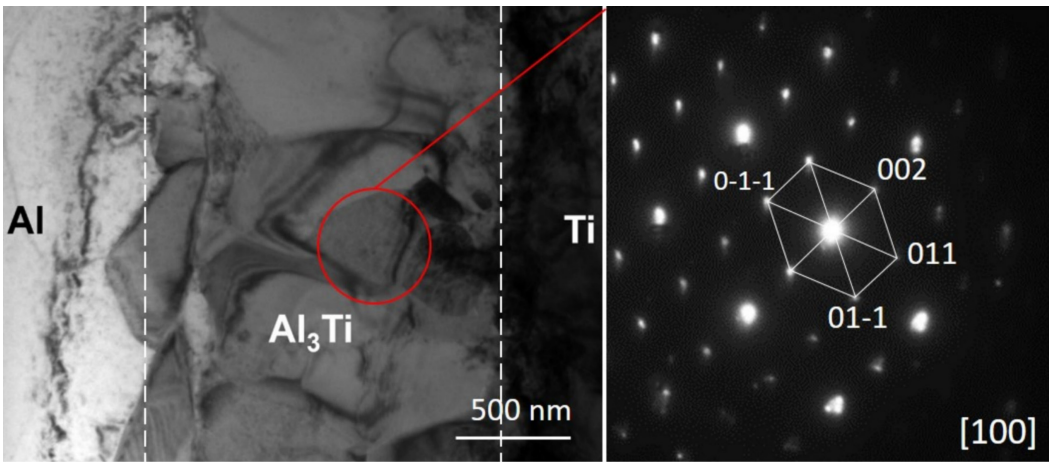

Fig. 6. TEM picture of the bonding zone in the sample annealed at 903 K (6th interface) for 1h with electron diffraction (SAED) pattern of theAl3Ti phase

$TiAl_3$, which indicates that the nucleation of $TiAl_3$ at the Ti/Al interface is most probable.

Fig. 7 shows SEM/BSE microstructure images presenting the cross sections of hot pressed Ti/Al sheets, reinforced with the ceramic powders. In all the samples, the intermetallic Al_3Ti phase was observed at both upper and lower interfaces. The coarse particles of Al_2O_3 (Fig. 7a) and the nanoparticles of SiC (Fig. 7b) were distributed between Al and the intermetallic layer. In this sample, coarse grains of Al_3Ti also occurred, but they were not accompanied by cracks. Opposed to that, the sample reinforced with the coarse (around 35 μm) SiC powder contained a number of cracks, in both the Al_3Ti layer and the Al area (Fig. 7c). These cracks may have resulted from the pressing of coarse ceramic particles and the brittle intermetallic phase. The Al foil used to produce this sample was too thin to compensate for the force action on Al_3Ti and ceramic particles. It is also possible that too much heat was generated at the interface, preventing the micro-melted areas from cooling and solidifying, a phenomenon reported by Loureiro et al. [10] and Zakharenko et al. [11]. Some parts of the interface did not contain intermetallic phases, a result of the presence of large grains of the ceramic layer, which blocked the reaction between the Ti and Al layers.

3.2. The Charpy impact test

The macroscopic images of the samples taken after the Charpy impact test were shown on Fig. 8a. All the samples tested were bent, but none was broken. Similar results were obtained by Bataev et al. [1] and Paul et al. [3], for Ti/Al multilayered clads obtained by explosive welding.

In almost all the samples strengthened with an additional ceramic layer, delamination was detected, indicating that all the ceramic powders increased the brittleness of the clads joined by the Al_3Ti phase. Breaking at the interface between the metal and intermetallic phases prevented the main crack from propagating across the whole cross-section. For the two samples made from Al foils V1 with a coarse Al_2O_3 powder layer and V2 with a coarse SiC layer the test was not conducted, due to partial delamination after hot pressing.

The results of the Charpy impact tests were shown on Fig. 8b and Table 6. The values are the average results of the tests carried out on the three specimens for each sample. The highest impact energy was observed for the U1 sample strengthened by additional Al_2O_3 layer. The Al_2O_3 particles with particle size about 10-20 μm and trigonal symmetry are located close to the

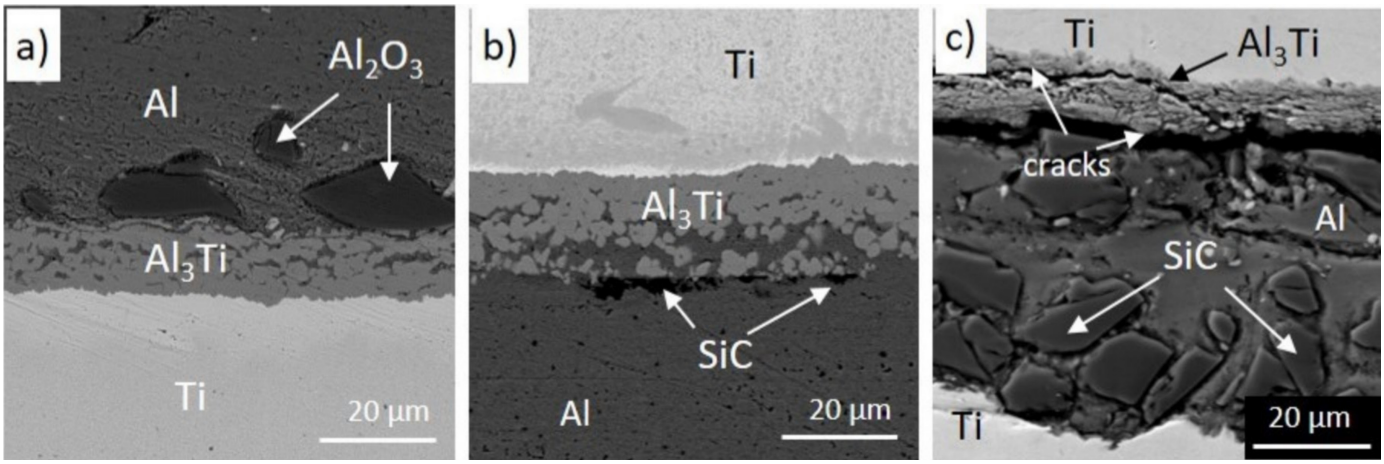

Fig. 7. SEM-BSE micrographs of Al-ceramic-Ti composites annealed at 903 K. Pictures were taken from the central part of the sample (7th interface)

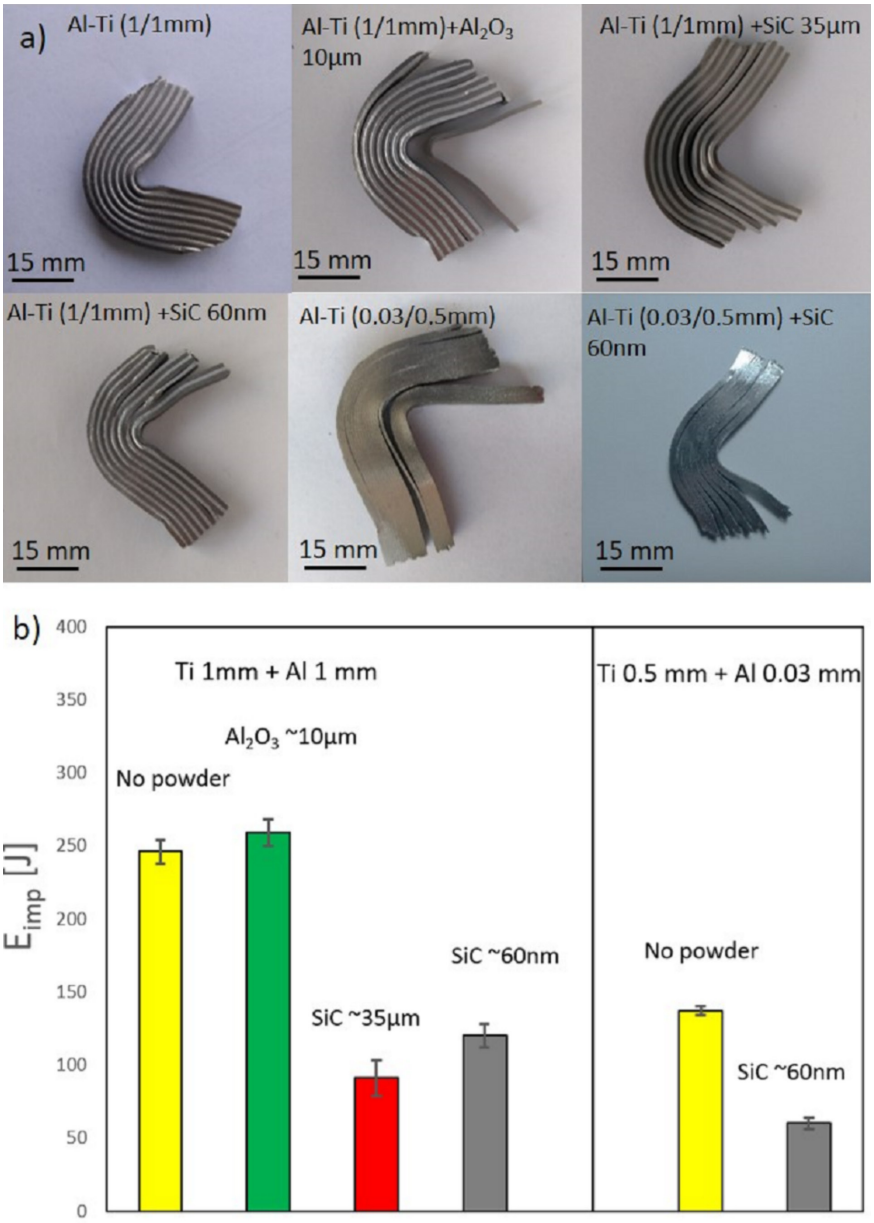

Fig. 8. a) The overall look of the Al-Ti clads after Charpy impact test, b) the values of the toughness of Al-Ti clads. The bar color corresponds to ceramic powder layer between Al and Ti plates

Al plate and some of them deeper inside the Al_3Ti layer (Fig. 7a). No cracks was observed on the SEM pictures, which may explain the good mechanical properties. Also the distribution of Al_2O_3 particles is more or less uniform. On the other hand, the lowest impact energy was observed for the for the Al-SiC-Ti clads (U2, U2n and V2n). The coarse (~35 µm) SiC particles causes stress and formation of cracks inside the brittle Al_3Ti phase and delamination of Al plate from Al_3Ti phase, which was shown on Fig. 7c. The fine (~60 nm) SiC particles tend to become non-uniform distribution and clustering (Fig. 7b), which has a negative influence on the mechanical behaviors of the composites, what was mentioned earlier by Hashemi et a. [12].

The structure of the intermetallic Al_3Ti phase revealed to be similar in all samples annealed in a whole range of temperatures and times – the grains are coarse (about 700 nm) and nearly equiaxed. Thus the differences in the results of the Charpy impact test are not depends on the structure but because of the applied ceramic powder between Al and Ti clads.

Further annealing at temperatures higher than 903 K could result in the formation of other intermetallic phases, such as

TABLE 6

Results of Charpy impact test investigation. S_0 is the cross-section of the samples before test, E_{imp} is the impact Energy

Sample	S_0 [cm^3]	E_{imp} [J]
U0	0.75	246
U1	0.76	259
U2	0.73	91
U2n	0.73	120
V0	0.59	137
V2n	0.59	61

AlTi and Al_2Ti [13]. The presence of these phases can significantly improve the ballistic performance of Al-Ti composites, but this improvement would not be achieved without further heat treatment of clads containing the Al_3Ti phase. This phase will react with Ti at temperatures higher than 903 K, and a new intermetallic will form.

4. Conclusions

Hot pressing under air atmosphere showed to be an effective technology for producing Ti/Al multilayered sheets strengthened with ceramic particles, and one not requiring any special or expensive equipment. Producing Al-Ti multilayered composites requires pressing to be carried out in a temperature close to the Al melting point but not too close, since it might result in leaking Al out of the clads. The STEM/EDX examinations revealed that the plates were not oxidized, as the pressure applied to them prevented reaction between the metal and oxygen. The SEM/BSE measurements showed that the thickness of an intermetallic layer increased with the annealing time and temperature. In the lowest temperature of 823 K, this layer's thickness varied from 0.6 μm for 1 hour to 1.2 μm for 10 hours of annealing; in the highest temperature of 903 K, however, it ranged from 2.4 μm for 1 hour to almost 12 μm for 10 hours of annealing. The TEM microstructure observations backed up by the SAED and EDX analyses revealed the presence of only the Al_3Ti phase inside the intermetallic layer, a similar observation to that observed in the composites produced through explosive welding technology. The structure of the Al_3Ti phase was coarse-grained with a grain size of about 700 nm. This has been confirmed by the STEM and TEM analyses. The growth rate constant ranged from about 0.5 $\mu m/h^n$ in 823 K to 2.3 $\mu m/h^n$ in 903 K.

The Charpy impact tests revealed a high ductility of the composites, as none of the samples broke during testing. The delamination of the composites was problematic, because their high brittleness increased with the quantity of the ceramic powder. The problem occurred to be particularly serious when the powder with coarse particles (10-35 mm) was used. Two composites made with thin Al foils and the coarse powder layer V1 and V2 delaminated after the pressing process. The microstructure of Al_3Ti should have no influence to the results of Charpy impact test, because is similar to all samples annealed in all heating conditions – the grains are coarse and nearly equiaxed.

The highest impact energy was observed for the sample with additional Al_2O_3 layer (U1), which points to their highest ductility. The Charpy impact test exhibits the lowest impact energy for Al-SiC-Ti composites, indicating their low plasticity.

Acknowledgements

This work was supported by the National Science Centre of Poland in the frame of the project no. 2016/21/B/ST8/00462.

REFERENCES

[1] I.A. Bataev, A.A. Bataev, V.I. Mali, D.V. Pavliukova, Structural and mechanical properties of metallic-intermetallic laminate composites produced by explosive welding and annealing, Mater. Design **35**, 225-234 (2012). DOI: https://doi.org/10.1016/j.matdes.2011.09.030

[2] F. Foadian, M. Soltanieh, M. Adeli, M. Etminanbakhsh, A Study on the Formation of Intermetallics During the Heat Treatment of Explosively Welded Al-Ti Mulitlayers, Metall. Mater. Trans. A **45A**, 1823 (2014). DOI: https://doi.org/10.1007/s11661-013-2144-6

[3] H. Paul, Ł. Maj, M. Prażmowski, A. Gałka, M. Miszczyk, P. Petrzak, Microstructure and mechanical properties of multilayered Al/Ti composites produced by explosive welding, Procedia Manufacturing **15**, 1391-1398 (2018). DOI: https://doi.org/10.1016/j.promfg.2018.07.343

[4] D.M. Fronczek, R. Chulist, Z. Szulc, J. Wojewoda-Budka, Growth kinetics of $TiAl_3$ phase in annealed Al/Ti/Al explosively welded clads, Mater. Lett. **198**, 160-163 (2017). DOI: https://doi.org/10.1016/j.matlet.2017.04.025

[5] F. Kong, Y. Chen, D. Zhang, Interfacial microstructure and shear strength of Ti-6Al-4V/TiAl laminate composite sheet fabricated by hot packed rolling, Mater. Design **32**, 3167-3172 (2011). DOI: https://doi.org/10.1016/j.matdes.2011.02.052

[6] H. Xiao, Z. Qi, C. Yu, C. Xu, Preparation and properties for Ti/Al clad plates generated by differential temperature rolling, J. Mater. Process. Tech. **249**, 285-290 (2017). DOI: https://doi.org/10.1016/j.jmatprotec.2017.06.013

[7] M. Fan, Z. Luo, Z. Fu, X. Guo, J. Tao, Vacuum hot pressing and fatigue behaviors of Ti/Al laminate composites, Vacuum **154**, 101-109 (2018). DOI: https://doi.org/10.1016/j.vacuum.2018.04.047

[8] L. Qin, M. Fan, X. Guo, J. Tao, Plastic deformation behaviors of Ti-Al laminated composite fabricated by vacuum hot-pressing, Vacuum **155**, 96-107 (2018). DOI: https://doi.org/10.1016/j.vacuum.2018.05.021

[9] J. Li, K.H. Wang, K. Zhang L.L. Kang, H. Liang, Mechanism of interfacial reaction between Ti and Al-ceramic, Mater. Design **105**, 223-233 (2016). DOI: https://doi.org/10.1016/j.matdes.2016.05.073

[10] G.H.S.F.L. Carvalho, I. Galvão, R. Mendes, R.M. Leal, A. Loureiro, Explosive welding of aluminium to stainless steel, J. Mat. Process. Tech. **262**, 340-349 (2018). DOI: https://doi.org/10.1016/j.jmatprotec.2018.06.042

[11] I. D. Zakharenko, Critical conditions in detonation welding, Fizika Goreniya i Vzryva **8** (3), 422-427 (1972).

[12] M. Tayyebi, D. Rahmatabadi, M. Adhami, R. Hashemi, Influence of ARB technique on the microstructural, mechanical and fracture properties of the multilayered Al1050/Al5052 composite reinforced by SiC particles, J. Mater. Res. Tech. **8** (5), 4287-4301 (2019). DOI: https://doi.org/10.1016/j.jmrt.2019.07.039

[13] M.N. Yuan, Lili Li, Zh J. Wang, Study of the microstructure modulation and phase formation of Ti-Al_3Ti laminated composites, Vacuum **157**, 481-486 (2018). DOI: https://doi.org/10.1016/j.vacuum.2018.09.002